AGU PUBLICATIONS

JGR

Journal of Geophysical Research: Biogeosciences

RESEARCH ARTICLE
10.1002/2016JG003527

Key Points:
- Hyporheic zone expands and contracts with seasonal snowmelt cycle
- At depths where groundwater influence fluctuates, the microbial community is unique
- River-groundwater mixing is the main control on microbial community structure

Supporting Information:
- Supporting Information S1

Correspondence to:
M. J. Wilkins,
wilkins.231@osu.edu

Citation:
Danczak, R. E., A. H. Sawyer, K. H. Williams, J. C. Stegen, C. Hobson, and M. J. Wilkins (2016), Seasonal hyporheic dynamics control coupled microbiology and geochemistry in Colorado River sediments, *J. Geophys. Res. Biogeosci.*, *121*, 2976–2987, doi:10.1002/2016JG003527.

Received 21 JUN 2016
Accepted 7 NOV 2016
Accepted article online 18 NOV 2016
Published online 3 DEC 2016

Seasonal hyporheic dynamics control coupled microbiology and geochemistry in Colorado River sediments

Robert E. Danczak[1], Audrey H. Sawyer[2], Kenneth H. Williams[3], James C. Stegen[4], Chad Hobson[3], and Michael J. Wilkins[1,2]

[1]Department of Microbiology, Ohio State University, Columbus, Ohio, USA, [2]School of Earth Sciences, Ohio State University, Columbus, Ohio, USA, [3]Earth and Environmental Sciences, Lawrence Berkeley National Laboratory, Berkeley, California, USA, [4]Biological Sciences Division, Pacific Northwest National Laboratory, Richland, Washington, USA

Abstract Riverbed microbial communities play an oversized role in many watershed ecosystem functions, including the processing of organic carbon, cycling of nitrogen, and alterations to metal mobility. The structure and activity of microbial assemblages depend in part on geochemical conditions set by river-groundwater exchange or hyporheic exchange. To assess how seasonal changes in river-groundwater mixing affect these populations in a snowmelt-dominated fluvial system, vertical sediment and pore water profiles were sampled at three time points at one location in the hyporheic zone of the Colorado River and analyzed by using geochemical measurements, 16S rRNA gene sequencing, and ecological modeling. Oxic river water penetrated deepest into the subsurface during peak river discharge, while under base flow conditions, anoxic groundwater dominated shallower depths. Over a 70 cm thick interval, riverbed sediments were therefore exposed to seasonally fluctuating redox conditions and hosted microbial populations statistically different from those at both shallower and deeper locations. Additionally, microbial populations within this zone were shown to be the most dynamic across sampling time points, underlining the critical role that hyporheic mixing plays in constraining microbial abundances. Given such mixing effects, we anticipate that future changes in river discharge in mountainous, semiarid western U.S. watersheds may affect microbial community structure and function in riverbed environments, with potential implications for biogeochemical processes in riparian regions.

1. Introduction

The hyporheic zone is the shallow streambed region where surface water and groundwater mix. Strong geochemical gradients along hyporheic and groundwater flow paths support significant biogeochemical activity and a wide variety of macrofauna, with capabilities ranging from filtering organic material to acting as a food source for higher organisms such as predatory fish and invertebrates [*Boulton et al.*, 2010; *Krause et al.*, 2011]. Further down the food web, metabolically active microorganisms in this zone drive transformations of both river water and groundwater, with implications for carbon processing, nutrient cycling, and contaminant mobility [*Feris et al.*, 2004; *Fischer et al.*, 2005; *Febria et al.*, 2010, 2012; *Stegen et al.*, 2016]. Key controls on the extent of these biogeochemical transformations in the hyporheic zone include water residence times that may range from minutes to years [*Zarnetske et al.*, 2011; *McCallum and Shanafield*, 2016], chemical concentrations, and the presence and activity of diverse microbial functional guilds [*Febria et al.*, 2012]. Residence times are relatively shorter for faster hyporheic flows, which generally occur where river velocity is fast, bed form submergence is low, and streambed permeability is high [*Zarnetske et al.*, 2011]. Residence times are also modulated by the rate of ambient groundwater discharge, with rapid discharge restricting the depth of hyporheic mixing and eliminating deeper hyporheic flow paths [*Cardenas and Wilson*, 2007; *Cardenas*, 2009; *Hester et al.*, 2013].

Diverse groups of microorganisms within the hyporheic zone play direct roles in metabolizing specific carbon pools [*Findlay et al.*, 1993; *Fischer et al.*, 2002; *Stegen et al.*, 2016], mobilizing metals and metalloids [*Nagorski and Moore*, 1999; *Xie et al.*, 2014; *Hartland et al.*, 2015], and reducing oxidized nitrogen species [*Storey et al.*, 2004; *Fischer et al.*, 2005]. While metal concentrations are inferred to exert strong controls on microbial community composition in metal-contaminated hyporheic zone sediments [*Feris et al.*, 2003], in other regions, carbon supply and form are important variables in constraining microbial activity [*Wagner et al.*, 2014]. In some locations a significant fraction of hyporheic zone respiration is supported by stream-derived dissolved organic carbon (DOC). Where hyporheic zones are dominated by fine silt- and clay-rich sediments,

stream-sourced DOC may not penetrate far into the hyporheic zone due to permeability constraints, and organic matter in sediments may be a primary source of DOC [*Battin et al.*, 2003]. Despite these studies, little is understood about how temporal dynamics in hyporheic mixing influence riverbed microbial communities and associated biogeochemical processes.

Hyporheic zones in semiarid western U.S. watersheds represent ideal locations to study dynamic processes that link hydrology, geochemistry, and microbiology. Snowmelt dominates river discharge in these regions. Indeed, in the Upper Colorado River Basin (UCRB), snowmelt from the mountains of Wyoming and Colorado sources 85–90% of discharge, which is mostly delivered during spring months [*Miller et al.*, 2014]. At our study site on the upper, free-flowing portion of the Colorado River near Rifle, CO, river discharge varies by over an order of magnitude between base flow and peak flow. Previous work on the adjacent floodplain has demonstrated that these river stage fluctuations are large enough to have significant effects on subsurface microbial community structure and redox conditions [*Danczak et al.*, 2016]. We hypothesized that these seasonal fluctuations in discharge would cause hyporheic zone expansion during peak flow and contraction during base flow, with implications for redox geochemistry and associated microbial communities in the riverbed. Such changes may be especially important in the UCRB, where groundwater chemistry is particularly distinct from river water chemistry and characterized by high salinity and metal concentrations due to the underlying Mancos shale [*Morrison et al.*, 2012]. Seasonal changes to the biogeochemical structure and function of the hyporheic zone may have a profound influence on solute loads from groundwater to the river, since upwelling groundwater passes through the reactive hyporheic zone before discharging to the river.

Here we report depth-resolved observations of hyporheic zone geochemistry and microbial community structure at three time points spanning the seasonal hydrograph excursion for the Colorado River near Rifle, CO. Vertical profiles of pore waters and sediments collected at one location were used to determine (1) the extent of temporal hyporheic zone expansion and contraction and (2) the effect of such hydrologic perturbations (i.e., hyporheic mixing) on microbial community structure and inferred hyporheic zone biogeochemical processes (i.e., redox cycling) in the riverbed. These results offer rare insight into coupled hydrological, geochemical, and microbiological processes accompanying dynamic hyporheic mixing and may assist in modeling efforts to predict perturbations to the biogeochemical function of hyporheic zones as climate change influences snowmelt and river discharge in the UCRB.

2. Methods

2.1. Sampling Site and Protocol

Depth-resolved pore water samples across the zone of hyporheic mixing were collected adjacent to a well-studied riparian floodplain outside of Rifle, CO (described extensively in *Williams et al.* [2011]) (Figure 1a) during spring flood, summer base flow, and winter base flow periods in the Colorado River between 2014 and 2015 (Figure 1b). Grain sizes, and thus hydraulic conductivity at our sampling location, are likely similar to those measured in the adjacent riparian zone by *Yabusaki et al.* [2011], as all these materials are derived from river depositional processes. Aquifer sediments are dominated by muddy- and sandy-gravels (56–92%), with a smaller component of fine particulates. The three sampling time points are referred to as Spring (high river discharge in May 2014), Summer (base flow during August 2014), and Winter (base flow in January 2015) (Figure 1b). Portable pore water sippers (MHE products, MI) were progressively driven into the riverbed at 10 cm vertical resolution to recover pore fluids (~60–100 mL volume at each depth) after purging the sipper internal volume, which were immediately filtered through a Sterivex filter (0.2 μm) (Millipore, MA, USA). May samples were collected with a 100 cm long sipper, while August and January samples were collected with a 200 cm long sipper, resulting in deeper hyporheic zone profiles. Filtered pore fluids were preserved for anion, cation, and organic/inorganic carbon analyses in glass bottles and stored at 4°C. Filters were immediately frozen at −80°C and shipped back to the Ohio State University on dry ice for DNA extraction.

2.2. Hydrology

To monitor changes in river stage and river-aquifer connections, water levels were recorded hourly in a stilling well approximately 4 km upstream and in multiple wells in the adjacent floodplain (Figure 1a). Floodplain wells have an outer diameter of 10.8 cm and typical screen length of 4.5 m. Screens are generally positioned

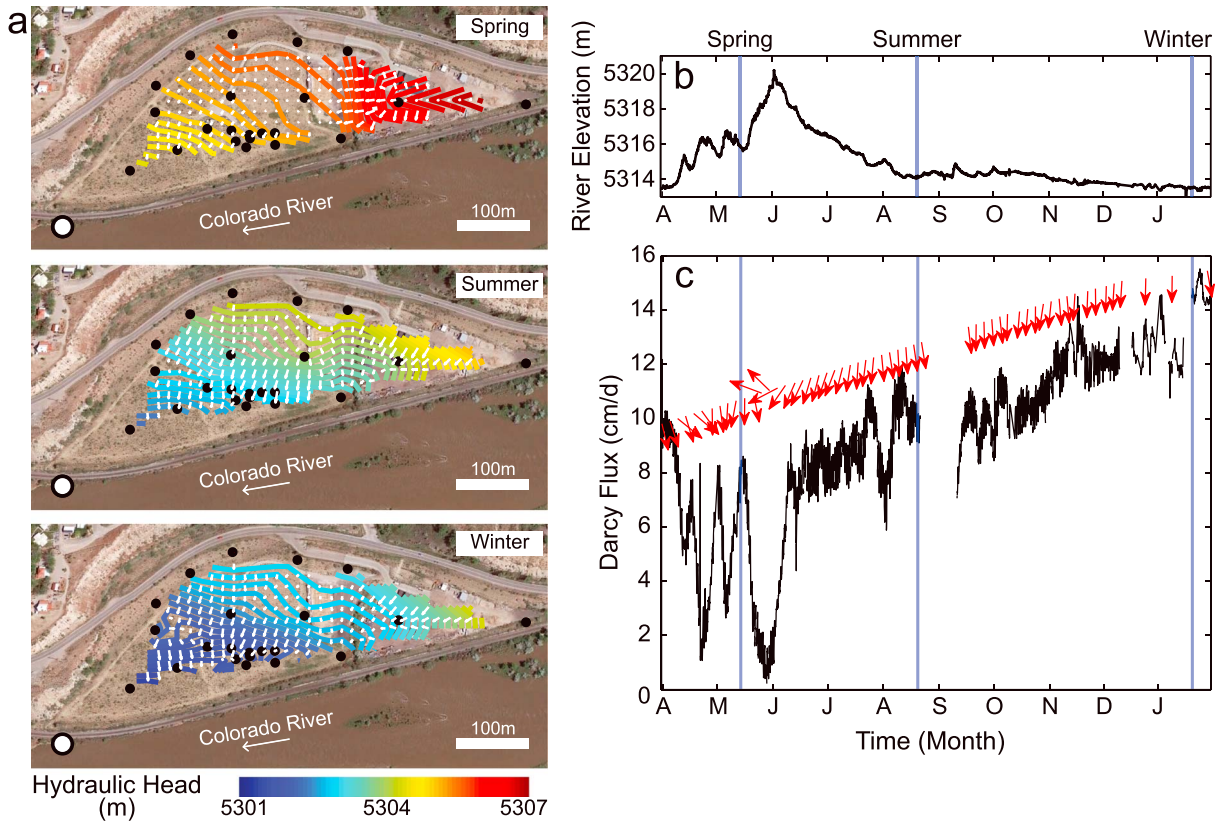

Figure 1. (a) Map of hydraulic head in the floodplain aquifer across three sampling seasons. Samples for this study were collected at the location marked by a white circle. The black dots indicate groundwater monitoring well locations used for hydrologic calculations. (b) River stage hydrograph for the Colorado River with sampling times indicated by blue lines. (c) Magnitude (black line) and direction (red arrows) of Darcy flux through the floodplain aquifer near the sampling location based upon local hydraulic head calculations. Groundwater flow is generally south toward the river.

between 4 and 7 m below the land surface. Hydraulic heads in floodplain wells were used to map the water table elevation during the three sample dates and interpret flow directions in the shallow floodplain aquifer. Specifically, three wells near the sampling location were selected for continuous triangulation of hydraulic head gradients over a 10 month period spanning the three sampling dates (the river stilling well was too far from the site to use in triangulation). The magnitude and direction of specific discharge, or Darcy velocity, were calculated from the hydraulic head gradient according to Darcy's law, assuming a floodplain aquifer hydraulic conductivity of 3.5×10^{-4} cm/s [*Yabusaki et al.*, 2011].

2.3. Geochemical Analysis

Chloride and sulfate concentrations were measured by using an ion chromatograph (ICS-2100 Dionex, CA, USA) equipped with an AS-18 analytical column. Total dissolved iron concentrations were determined by using inductively coupled plasma–mass spectrometry equipped with a dynamic reaction cell (ICP-DRC-MS) (PerkinElmer-Sciex ELAN 6100 DRC^{plus} ICP-MS, PerkinElmer, Waltham, MA, USA). Total carbon (TC) and nonpurgeable organic carbon (NPOC) were measured on a TOC-LCPN instrument (Shimadzu, MD, USA). Dissolved inorganic carbon (DIC) was calculated through the difference in TC and NPOC. Technical replicate standard deviations were plotted as error bars for DIC, NPOC, and iron.

Chloride was used as a conservative tracer to assess mixing between river water and groundwater end-members as a function of depth within the riverbed on each sampling date. Specifically, the fraction of river water at each depth was calculated as $(C(z) - C_g)/(C_r - C_g)$, where $C(z)$ is the chloride concentration at depth of interest, C_r is the chloride concentration of river water, and C_g is the chloride concentration at the deepest pore water sample. Although the deepest pore water sample was only 100 cm in May (as opposed to 200 cm in August and January), C_g was similar on all three dates (4.04 mM, 3.07 mM, and 3.10 mM).

Furthermore, chloride concentrations for the deepest sampling depths were comparable with previous studies in the adjacent floodplain (between 3 and 6 mM) [*Danczak et al.*, 2016]. For comparison, C_r was far more dynamic and ranged from 1.28 mM to 5.54 mM for May and January, respectively. For this study, we define the hyporheic zone as the interval that contains at least 20% river water. Conversely, pore water samples with less than 20% river water are considered groundwater. We use the percentage of river water as our primary indicator of "mixing."

2.4. 16S rRNA Gene Processing

DNA was extracted from Sterivex filters by using the Powersoil DNA Isolation Kit (MoBio Laboratories, Inc., Carlsbad, CA, USA). Final DNA concentrations were determined by using a Qubit Flurometer (Invitrogen, Carlsbad, CA, USA). The V4 region of 16S rRNA genes was amplified and sequenced by using the bacterial/archaeal primer set 515 F/806R on an Illumina MiSeq instrument at the Argonne National Laboratory. Resulting reads were processed through the QIIME pipeline (V1.7.0) and clustered into operational taxonomic unit (OTU) classifications at 97% similarities. 16S rRNA gene sequences from adjacent aquifer groundwater samples were collected as part of a concurrent investigation and were included in microbial community analyses [*Danczak et al.*, 2016].

2.5. Data Analyses

Alpha diversity within each microbial community sample (16S rRNA gene data) was determined via Shannon diversity calculations [*Shannon*, 1948] (diversity, vegan package v2.21), while beta diversity was calculated by using Bray-Curtis dissimilarity [*Bray and Curtis*, 1957]. From these dissimilarities, community differences between sampling depth and time were examined in R v3.1.2 through nonmetric multidimensional scaling (NMDS) (metaMDS) and compared by using global and pairwise PERMANOVA (adonis, vegan package v2.2.1). A posteriori SIMPER analysis was performed in R (simper, vegan package v2.2.1) to identify community members significantly contributing to between-sample differences. The species scores for community members exhibiting the strongest influence (44 OTUs) were then plotted on the NMDS to visualize the relative contributions from each member to sample separation. To ensure valid NMDS distribution patterns, a detrended correspondence analysis was performed in R (decorana, vegan package v2.2.1) (Figure S1 in the supporting information). A constrained redundancy analysis was additionally calculated (rda, vegan package v2.2.1) to better demonstrate the factors contributing to microbial community differences.

2.6. Ecological Modeling

To investigate potential ecological drivers within this system, ecological modeling was performed following the protocol outlined in *Stegen et al.* [2015]. As per the protocol, a phylogenetic signal was first found to establish a link between phylogeny and ecology by using depth as the environmental variable for calculating niche differences. Next, the β-mean nearest taxon distance (βMNTD) was calculated for each possible pairwise comparison between samples in order to better understand community composition. Using 999 community randomizations to create null models, β-nearest taxon index (βNTI) was calculated to determine the deviation of the observed βMNTD from the null βMNTD. The resulting βNTI values were interpreted to understand the phylogenetic turnover through depth or time providing insight into whether deterministic (i.e., selection) or stochastic (i.e., random) processes shaped the community. If a $|\beta\text{NTI}|$ value exceeds 2, a deterministic process is responsible for differences between microbial communities in two samples; conversely, if a $|\beta\text{NTI}|$ value is less than 2, a stochastic process explains observed differences in microbial community composition between two samples [*Stegen et al.*, 2012]. Stochastic processes might include random cell deaths or limitations in cell dispersal within a particular habitat, for example. Conversely, deterministic forces include abiotic parameters that might select for specific microorganisms (e.g., localized abundances of certain nutrients) and drive microbial community structure toward a particular composition. Deterministic processes can be further categorized as either variable selection or homogenizing selection. Variable selection occurs when two communities are more dissimilar than would be expected by random chance and occurs if βNTI is greater than 2. Typically, these processes occur when the environmental conditions between the compared communities are very different (e.g., large concentration differences in NPOC) resulting in different compositions [*Stegen et al.*, 2016]. If βNTI is less than -2, communities are more similar than could occur by random chance and homogenizing selection is considered the dominant process. This type of selection typically occurs in situations where relatively constant environmental conditions push

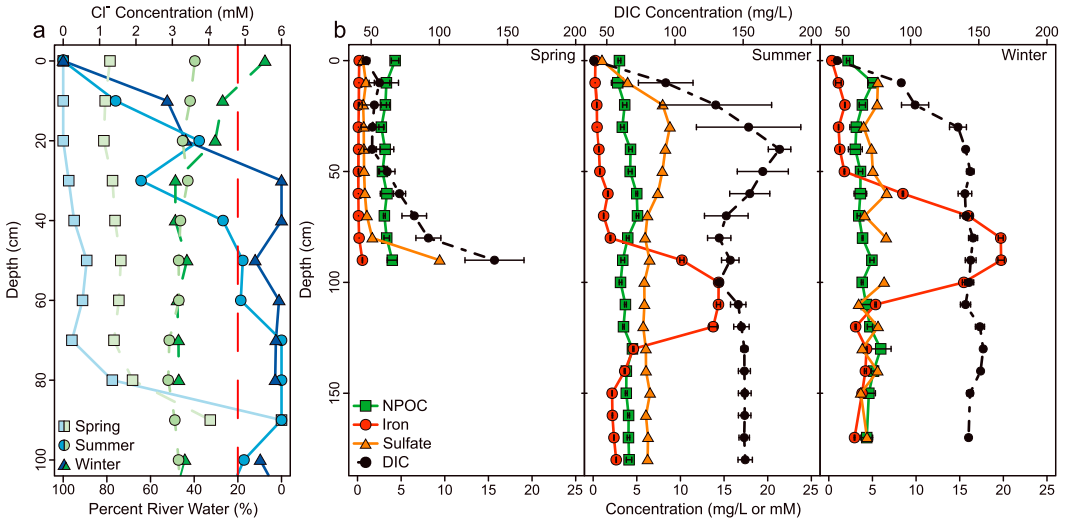

Figure 2. (a) Mixing dynamics (blue) and chloride concentrations (green) through the top 100 cm of the riverbed across the three seasons (Spring, Summer, and Winter); the red line indicates the percentage where water dominance transitions from river water to groundwater. (b) Depth profiles of concentrations for nonpurgeable organic carbon (NPOC), total iron, sulfate (bottom axis), and dissolved inorganic carbon (DIC) for each of the seasons (top axis).

community structure toward a common composition, such as in the case of microbial community succession in geochemically stable soil environments [*Dini-Andreote et al.*, 2015].

Environmental parameters (Fe, SO_4^{2-}, mixing, NPOC, and DIC) were regressed against the βNTI values in R (rcorr, Hmisc package v3.15) to elucidate which nonbiological factors may be responsible for observed differences in microbial community structures.

3. Results and Discussion

3.1. Hydrology and Geochemistry

Among the three sampling dates in May, August, and January, river stage was highest in May and lowest in January. Over all three seasons, groundwater in the floodplain generally flowed toward the river (azimuths ~220° to ~180°), as previously reported [*Williams et al.*, 2011] (Figure 1). Reversals in flow from the river to aquifer were brief and only occurred during periods of highest river stage in June (Figure 1). The rate of groundwater discharge to the river was lowest (7.9 cm/d) during May when the river stage was high. As stage fell through summer and fall, the groundwater discharge rate increased to 9.9 cm/d on the August sampling date and 14.6 cm/d on the January sampling date (Figure 1). Hydrodynamics in the floodplain aquifer are tightly linked with river stage dynamics [*Francis et al.*, 2010; *Nowinski et al.*, 2012], with associated impacts on aquifer biogeochemistry that are described in more detail in *Danczak et al.* [2016].

As the rate of groundwater discharge increased across the three sampling dates, the depth of hyporheic mixing decreased as determined by chloride concentration data (Figure 2a). During May, the hyporheic zone extended to 80 cm below the sediment-water interface. During August and January, the hyporheic zone only extended to 40 cm and 20 cm, respectively. These observations are consistent with modeled responses of hyporheic zones to ambient groundwater discharge [*Cardenas*, 2009; *Sawyer and Cardenas*, 2012; *Boano et al.*, 2014]: groundwater restricts the depth of mixing and also shortens hyporheic residence times. Concentrations of chloride, dissolved inorganic carbon (DIC), and sulfate tracked mixing dynamics (Figure 2b). DIC was generally greater in groundwater than river water, and vertical gradients in DIC became steeper from May to January. Vertical sulfate concentrations increased at shallower depths in conjunction with decreased river water influence. Although we lack direct measurements of dissolved oxygen concentrations, the depth of the aerobic zone likely also decreased from May to January, as increasing discharge of suboxic groundwater would have restricted the depth of hyporheic mixing. Overall, these trends indicate that the upper ~80 cm of riverbed sediments likely undergo seasonal redox fluctuations driven by changes in the depth of hyporheic mixing and associated dominance of suboxic groundwater or oxic river water.

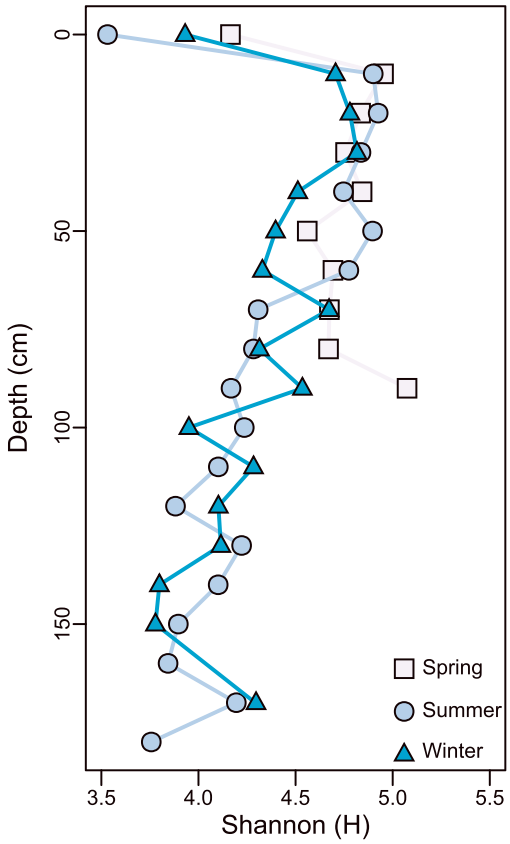

Figure 3. "Within-sample" Shannon diversity measurements across seasonal time points and depth profiles through the riverbed.

Total dissolved iron (likely Fe^{2+}) pore water profiles reflect inferred seasonal redox fluctuations in the riverbed environment. Greater concentrations of dissolved iron were detected in groundwater-dominated samples (Figure 2b), indicating that enzymatic Fe^{3+} reduction is an active process in portions of the riverbed that undergo seasonal fluctuations between oxic and anoxic conditions. During peak river discharge when the hyporheic zone expands, increased oxygen supply to deeper sediments could potentially generate fresh, bioavailable iron oxyhydroxide phases for later enzymatic microbial reduction [*Lovley and Phillips*, 1986]. Fe^{2+} concentrations were consistently low along the entire pore water profile in May. During August and January, spikes in Fe^{2+} concentrations between 50 cm to 120 cm depth indicate the presence of a rising redox front, which further supports our interpretation of progressive development of anoxia in the riverbed with increasing groundwater discharge (Figure 2b). This trend may also reflect the depletion of bioavailable Fe^{3+} phases at greater depths or the onset of sulfidogenesis that titrates aqueous iron pools. Organic carbon (as NPOC) appears disconnected from hyporheic mixing dynamics and independently fluctuates across sampling time points and depths (between 2.2 and 6 mg/L), behavior that is likely linked to microbial oxidation of labile carbon pools and biomass production [*Fasching et al.*, 2016; *Stegen et al.*, 2016].

3.2. Microbiology

Microbial community responses were examined in conjunction with changes in river stage (Spring, Summer, Winter). Alpha diversity metrics (i.e., Shannon diversity; "within sample diversity") showed similar trends through time with high values in near surface samples that subsequently decreased with depth (Figure 3). This result indicates higher diversity in the upper 90 cm of riverbed sediments than in the river or deeper riverbed sediments. Microbial community data across the three sampling time points was split into 90 cm intervals (i.e., 10–90 cm and 100–180 cm) and examined by using nonmetric multidimensional scaling (NMDS) calculated from 16S rRNA gene data to examine beta diversity (i.e., Bray-Curtis, "between sample diversity") (Figure 4). Significant differences between groupings defined by river stage/depth were found by using PERMANOVA with the largest individual differences in community composition occurring between river water-dominated sediments (Spring) and deeper, groundwater dominated sediments at later time points (Summer and Winter) (Table 1). Conversely, the most similar microbial communities across the three time points were found between Summer and Winter samples, reflecting common geochemical profiles through the hyporheic zone at both these base flow periods. Further, the development of increasingly anoxic riverbed conditions during periods of low river discharge is reflected in microbial community change, with inferred increases in similarity between near-surface (10–90 cm) and deeper (100–180 cm) microbial communities during the transition from Summer to Winter time points (Table 1). In summary, Figures 3 and 4 illustrate that shallower depths in the riverbed harbored more diverse and dynamic microbial populations, relative to deeper locations that were consistently dominated by groundwater (i.e., 100–180 cm depth range).

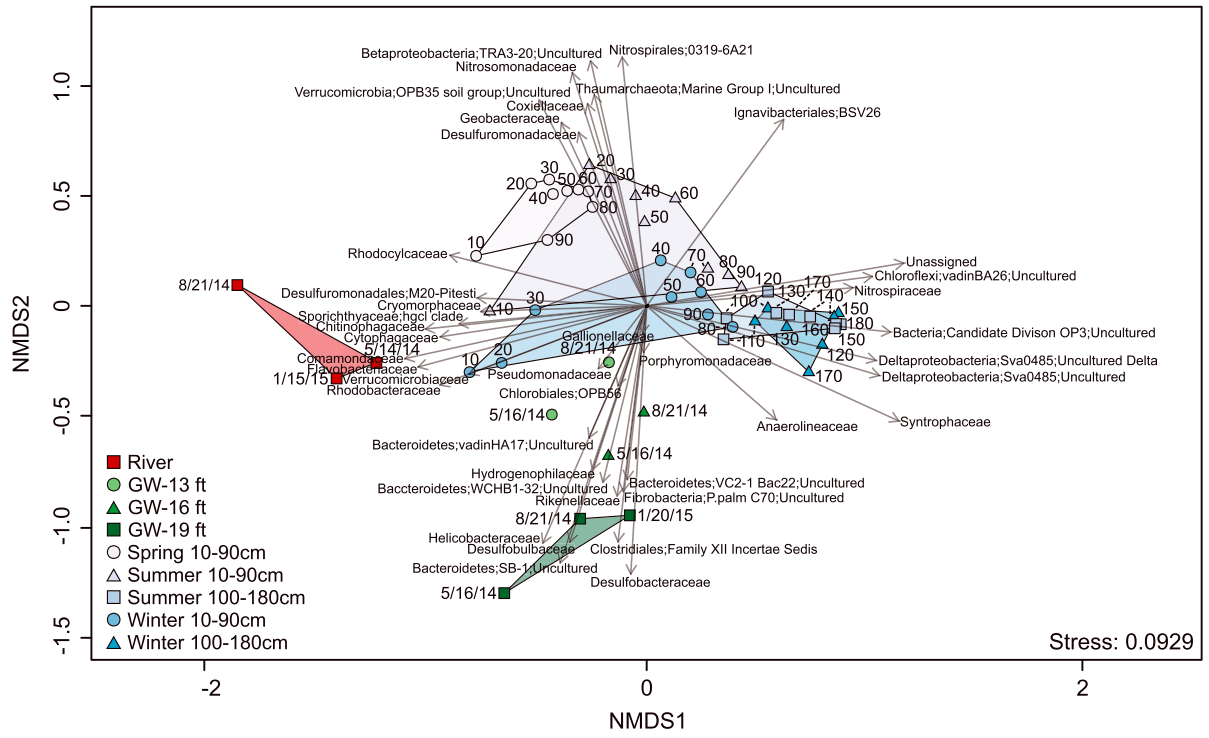

Figure 4. A nonmetric multidimensional scaling (NMDS) graph of microbial community 16S rRNA gene data. Each point is the community derived from one sample, and the distance between each point is related to the Bray-Curtis dissimilarity of the samples. The loading plot on top of the NMDS graph represents family-level community members that were determined by SIMPER analyses to be important in separating samples. The length and direction of each arrow vector are directly related to the degree of contribution to sample separation by a particular member. GW is the groundwater reference well sampled at three different depths (3.9624 m, 4.8768 m, and 5.7912 m) from the adjacent aquifer.

The presence of distinct microbial communities in riverbed zones that are exposed to annual redox fluctuations was inferred from multivariate ordination (Figure 4) and cluster analysis (Figure S2). Microbial populations found between 20 and 90 cm depths were distinguishable from those found in either of the chemical endmembers (river water and groundwater), highlighting the importance of dynamic geochemical conditions in shaping microbial community composition. SIMPER analyses were used to assess the importance of particular operational taxonomic units (OTUs) in driving dissimilarity between samples (Figure 4). Community members associated with shallower riverbed depths (10–20 cm) closely resemble OTUs that are found within river water samples both adjacent to this site and elsewhere (i.e., *Comamonadaceae*, *Rhodobacteraceae*, and *Chitinophagaceae*) [*Stegen et al.*, 2016], supporting geochemical inferences of river water intrusion into these sediments. Conversely, OTUs that affiliate with deeper depths tend to represent members typically found within groundwater at the site (i.e., *Syntrophaceae*, Candidate Division OP3) [*Danczak et al.*, 2016], reflecting the influence of groundwater on deeper riverbed sediments. Finally, distinguishing OTU signals are present

Table 1. PERMANOVA Results for Comparisons Between Each Season (Spring, Summer, and Winter) and Depth Group (i.e., 10–90 cm and 100–180 cm)[a]

	River	GW-13	GW-16	GW-19	Spring (10–90)	Summer (10–90)	Summer (100–180)	Winter (10–90)	Winter (100–180)
River		.	**	**	***	**	**	***	***
GW-13	5.550		*	**	*	*	*	*	***
GW-16	7.773	3.412		.	***	***	***	*	*
GW-19	8.742	4.543	2.082		**	**	**	***	*
Spring(10–90)	18.188	9.567	13.391	20.054		***	**	***	***
Summer(10–90)	9.682	3.688	4.556	8.865	6.864		***	.	***
Summer(100–180)	23.360	10.091	10.151	18.580	37.348	10.795		***	.
Winter(10–90)	7.056	2.646	2.892	6.611	9.848	2.600	8.145		***
Winter(100–180)	23.838	12.004	11.879	19.773	38.579	10.740	1.289	7.813	
Overall *F*-stat: 10.247						Significance: . >0.05 > * > 0.01 > ** > 0.001 > ***			

[a]Comparisons with groundwater (three depths) from the adjacent floodplain and river samples are also included.

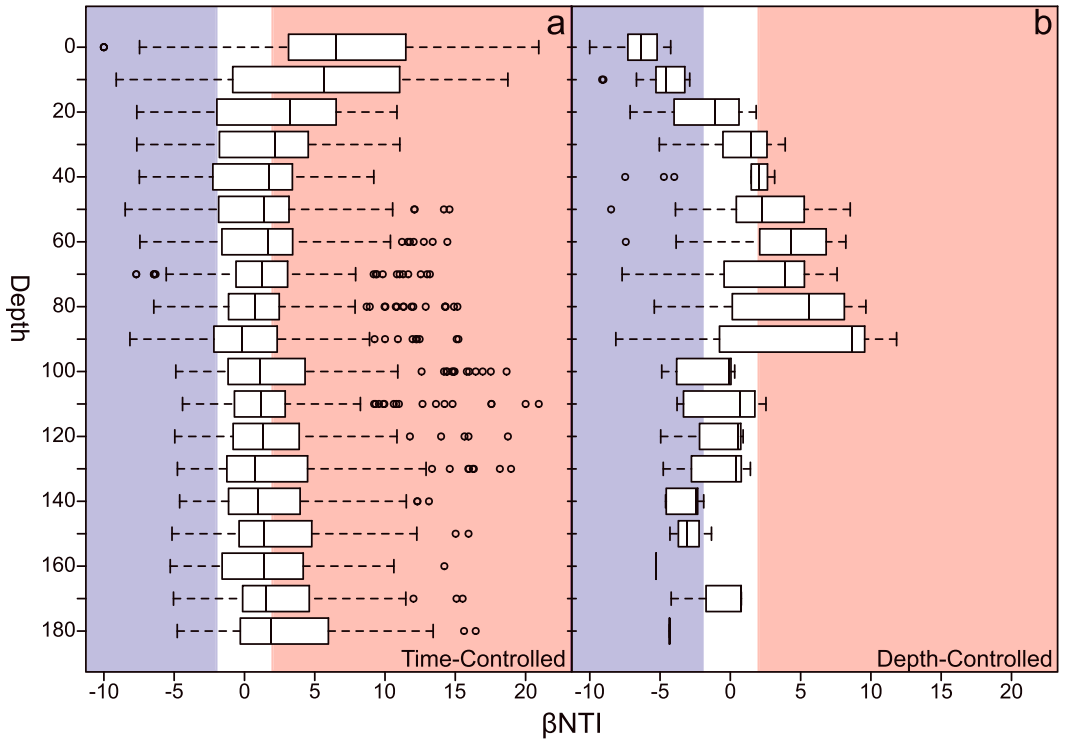

Figure 5. Overview of βNTI values illustrating trends through the depth profiles while controlling for (a) time and (b) depth. The blue-shaded region indicates βNTI values < -2 (homogenizing selection), while the red-shaded region indicates βNTI values > 2 (variable selection).

at depths where inferred annual redox cycling occurs (20–90 cm) (Figure 4). Included among these OTUs are signals for putative metal-reducing microorganisms (i.e., *Geobacteraceae*, and *Desulfuromonadaceae*); given that members of the *Geobacteraceae* have previously been implicated in metal reduction in alluvial sediments adjacent to our sampling location [*Holmes et al.*, 2002, 2013; *Wilkins et al.*, 2009], we suggest that these and other unidentified groups may play a similar role in the riverbed environment where they potentially contribute to the observed dissolved iron increases within this zone.

3.3. Ecological Modeling

To better understand the environmental constraints that shape microbial community composition within the riverbed environment, βNTI values were calculated to estimate the magnitude of either stochastic or deterministic ecological processes affecting microorganisms at a particular depth. Within this system, a significant phylogenetic signal over relatively short genetic distances was measured, allowing βNTI to be used to infer ecological processes (Figure S3). Analyses of all possible pairwise comparisons illustrate a wide distribution of βNTI values across the variable selection range, although values did peak within the stochastic region (between -2 and 2) (Figure S4). To compare appropriate samples, only pairwise comparisons between samples within a given time point (Time-Controlled) or at a given depth across time points (Depth-Controlled) were considered in subsequent analyses. Per the Time-Controlled depth comparisons, positive βNTI values (>2) indicative of variable selection decreased with increasing depth, subsequently stabilizing between -2 and 2 (stochastic range) at approximately 40 cm (Figure 5a). This trend indicates that at a given time point, hyporheic mixing drives dynamic geochemical conditions and controls microbial community structure in shallower sediments, relative to deeper, more stable locations.

Comparisons of samples from similar depths across time points (Depth-Controlled) revealed evidence for homogenizing selection (βNTI $<$ -2) in shallow zones that were dominated by river water at all three sampling times (e.g., 10 cm depth) (Figure 5b). This result, indicating that microbial communities at the sediment-water interface are extremely similar across time points, may be linked to the persistent influence of river water in this zone. Under such conditions, relatively constant geochemical parameters in river water (e.g., oxic

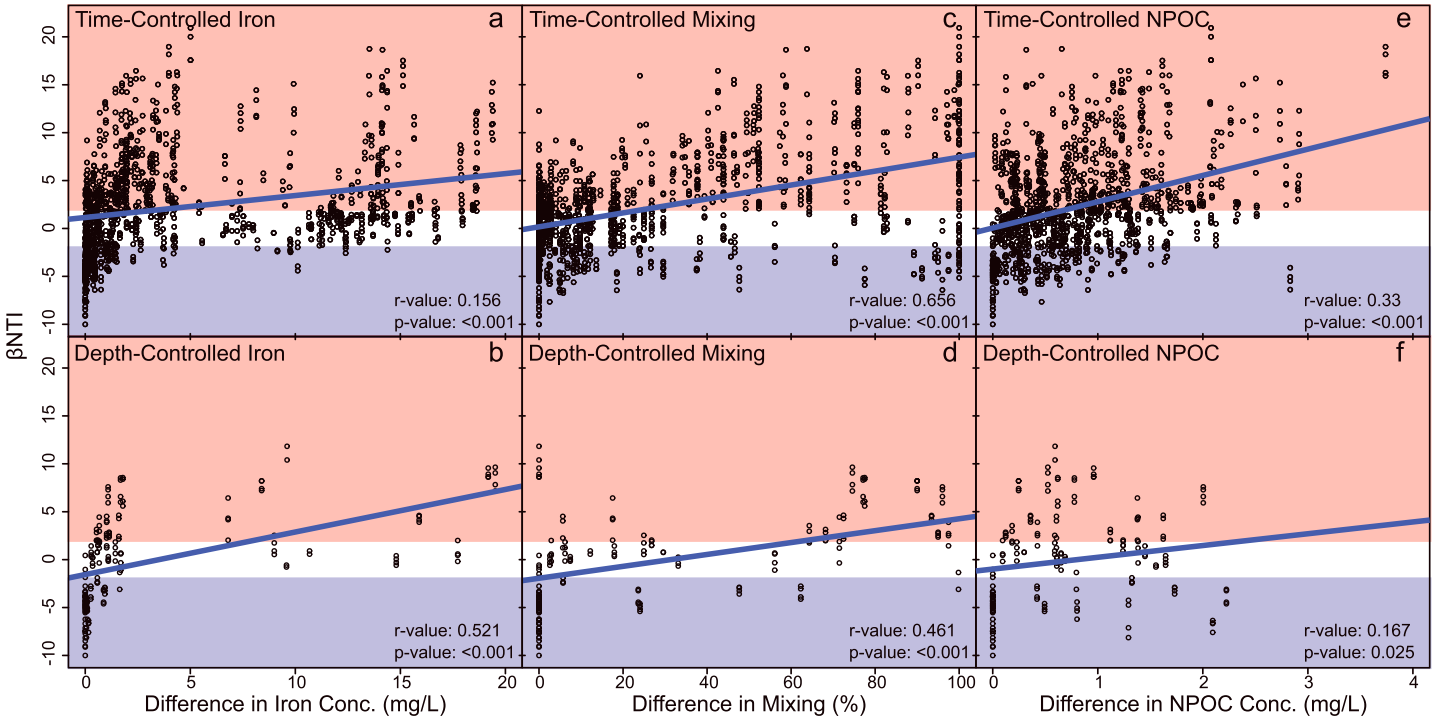

Figure 6. Correlations between environmental parameters and βNTI values under both time and depth controlled scenarios. (a) Time-controlled iron correlation, (b) depth-controlled iron correlation, (c) time-controlled mixing correlation, (d) depth-controlled mixing correlation, (e) time-controlled NPOC correlation, and (f) depth-controlled NPOC correlation. The blue-shaded region indicates βNTI values < -2 (homogenizing selection), while the red-shaded region indicates βNTI values > 2 (variable selection).

conditions and NPOC) exert the strongest controls on microbial community composition, resulting in this upper riverbed zone harboring the most similar microbial communities across seasonal time points [*Arntzen et al.*, 2006]. This result also indicates that dynamic parameters within Colorado River water which change depending upon the season (e.g., water temperature or chloride concentrations) (Figure 2b) have less of an effect in constraining microbial community structure in such near surface zones (e.g., 10 cm depth). Beneath this depth, however, βNTI values increased sharply across the region of inferred redox fluctuations, indicating that microbial community differences across time points in this zone were *greater* than that of random chance (Figure 5b). This pattern supports our suggestion that shallow hyporheic zone sediments (between 20 and 90 cm) are unique zones where dynamic mixing through time between river water and groundwater drives dynamic microbial populations.

Prior work in the adjacent floodplain during the same hydrologic perturbation revealed that there were significant linkages between hydrology and microbial community structure [*Danczak et al.*, 2016]. To understand which shifting hydrologic and geochemical parameters play a significant role in shaping the microbial communities in the hyporheic zone, correlations between βNTI values and geochemical concentrations were calculated. Although dissolved iron concentrations deviate significantly across vertical profiles (Figure 2b), this parameter is inferred to exert a relatively weak influence on microbial community structure (Figure 6a) within a single time point (e.g., Summer). A much stronger effect was detected when assessing correlations between larger differences in iron concentrations and βNTI values at a given depth across multiple time points (Figure 6b), indicating that fluctuations in Fe^{2+} through time are linked to differences between compared communities.

Strong correlations were also calculated between degree of river water mixing (% river water) and βNTI in both time-controlled and depth-controlled situations, indicating that mixing dynamics (and associated unmeasured variables) shape microbial community structure (Figures 6c and 6d). Finally, under time controlled situations (Figure 6e) NPOC concentration was a key predictor of variable selection, despite relatively small changes in bulk carbon concentrations within a depth profile (Figure 2b). This observation suggests that fine-scale changes in carbon composition and lability are partially responsible for measured community

differences [*Stegen et al.*, 2016], and supports previous studies that have reported hyporheic zone community composition changes driven by allochthonous carbon inputs [*Findlay et al.*, 2003; *Wagner et al.*, 2014]. Indeed, high-resolution mass spectrometry analyses have revealed significant differences in the composition of groundwater and river water carbon pools at this location (P. Mouser, personal communication). Under depth-controlled situations (Figure 6f) much weaker correlations between NPOC and βNTI were observed. Although an additional redundancy analysis supported the identification of many key constraints on microbial community structure (Figure S5), NPOC was not determined to explain significant community variance. This result highlights the greater sensitivity of the βNTI calculations in detecting controls (e.g., carbon lability within the NPOC pool) on community composition [*Stegen et al.*, 2013].

4. Conclusions

Results presented here indicate that snowmelt-driven Colorado River discharge likely causes significant fluctuations in hyporheic transport, redox behavior, and microbial community structure throughout the hyporheic zone. As river stage declines from spring runoff over summer and fall, increasing contributions from groundwater discharge reduce the depth of hyporheic mixing and allow reducing chemical conditions to develop at progressively shallower depths within the riverbed. As a result of these mixing dynamics a large interval within the riverbed (up to 70 cm deep) undergoes annual redox cycling between oxic river water dominated conditions and anoxic groundwater-dominated conditions. We posit that this redox cycling creates a highly reactive zone within the riverbed and significantly contributes to the oversized role that hyporheic processes play in the transformation of chemical species.

Measurements of microbial diversity indicated that this reactive zone contains a unique microbial population that can be clearly distinguished from those in both shallower and deeper locations in the riverbed environment. We suggest that dynamic conditions within this region select for microbial assemblages capable of diverse metabolisms, including aerobes that dominate during deeper river water-groundwater mixing and anaerobes during periods of dominant groundwater conditions. This inferred that metabolic flexibility linked to microbial diversity [*Petchey and Gaston*, 2002] within riverbed microbial populations is likely a significant factor that contributes to hyporheic zone reactivity, including the aforementioned reductive dissolution of iron oxyhydroxides.

Although patterns of end-member mixing were inferred to exert the greatest control on microbial assemblages, ecological models also indicated that fine-scale differences in organic carbon composition played a key role along depth profiles [*Wong and Williams*, 2010]. Bulk NPOC measurements performed in this study showed little spatial variation, suggesting that higher-resolution analyses of carbon pools are necessary to identify many of the substrates supporting microbial activity within riverbed environments. Although a series of studies have demonstrated that microorganisms utilized specific labile carbon pools under aerobic conditions [*Fischer et al.*, 2002; *Findlay et al.*, 2003], complementary experiments have not been performed over seasonal time points where hydrology drives fluctuating redox conditions.

Given that more efficient processing of carbon generally occurs under oxic conditions, the development of suboxic conditions in riverbed sediments are likely to have a significant impact on the extent of carbon utilization. Understanding such linkages is increasingly important given modeling predictions for the next 50 years in the UCRB, where warming temperatures and decreasing snowpack in the upper Colorado River basin will likely contribute to earlier snowmelt [*Adam et al.*, 2009; *Painter et al.*, 2010] and decreases in Colorado River discharge [*Ficklin et al.*, 2013] with base flow occurring for longer periods of the year [*Christensen and Lettenmaier*, 2007; *Tillman et al.*, 2016]. The loss of strong seasonal behavior and longer base flow periods will likely drive greater persistence of groundwater-dominated riverbed sediments. If the iron reduction identified during river base flow in this study is representative of the greater UCRB, longer periods of anoxic riverbed conditions may drive changes in metal mobilization and flux to the river channel via reductive dissolution and release of adsorbed metals, with implications for water quality [*Stucker et al.*, 2013; *Xie et al.*, 2014; *Hartland et al.*, 2015]. Less dynamic hydrologic behavior across the riverbed environment could result in lower microbial community diversity, with associated losses of functional potential. Despite the limited spatiotemporal scale of the analyses presented here, our results highlight the need to perform depth-resolved, long-term temporal hyporheic zone studies to improve our understanding of how climate change may lead to permanent alterations in the ecology and microbiology of riverbed environments.

Acknowledgments

This work was supported as part of the Genomes to Watershed Scientific Focus Area at Lawrence Berkeley National Laboratory, which is funded by the U.S. Department of Energy, Office of Science, Office of Biological and Environmental Research under award DEAC02-05CH11231. J.C.S. was supported by the U.S. Department of Energy (DOE), Office of Biological and Environmental Research, as part of Subsurface Biogeochemical Research Program's Scientific Focus Area at the Pacific Northwest National Laboratory (PNNL). PNNL is operated for the DOE by Battelle under contract DE-AC06-76RLO 1830. A portion of the research was performed by using Institutional Computing at PNNL. Supporting information is available at the journal website. 16S rRNA gene data from this study have been deposited at NCBI under bioproject number PRJNA31818.

References

Adam, J. C., A. F. Hamlet, and D. P. Lettenmaier (2009), Implications of global climate change for snowmelt hydrology in the twenty-first century, *Hydrol. Processes*, *23*(7), 962–972, doi:10.1002/hyp.7201.

Arntzen, E. V., D. R. Geist, and P. E. Dresel (2006), Effects of fluctuating river flow on groundwater/surface water mixing in the hyporheic zone of a regulated, large cobble bed river, *River Res. Appl.*, *22*(8), 937–946, doi:10.1002/rra.947.

Battin, T. J., L. A. Kaplan, J. D. Newbold, and S. P. Hendricks (2003), A mixing model analysis of stream solute dynamics and the contribution of a hyporheic zone to ecosystem function*, *Freshwater Biol.*, *48*(6), 995–1014, doi:10.1046/j.1365-2427.2003.01062.x.

Boano, F., J. W. Harvey, A. Marion, A. I. Packman, R. Revelli, L. Ridolfi, and A. Wörman (2014), Hyporheic flow and transport processes: Mechanisms, models, and biogeochemical implications, *Rev. Geophys.*, *52*, 603–679, doi:10.1002/2012RG000417.

Boulton, A. J., T. Datry, T. Kasahara, M. Mutz, and J. A. Stanford (2010), Ecology and management of the hyporheic zone: Stream–groundwater interactions of running waters and their floodplains, *J. North Am. Benthol. Soc.*, *29*(1), 26–40, doi:10.1899/08-017.1.

Bray, J. R., and J. T. Curtis (1957), An ordination of upland forest communities of southern Wisconsin, *Ecol. Monogr.*, *27*, 325–349.

Cardenas, M. B. (2009), Stream-aquifer interactions and hyporheic exchange in gaining and losing sinuous streams, *Water Resour. Res.*, *45*, W06429, doi:10.1029/2008WR007651.

Cardenas, M. B., and J. L. Wilson (2007), Exchange across a sediment-water interface with ambient groundwater discharge, *J. Hydrol.*, *346*, 69–80, doi:10.1016/j.jhydrol.2007.08.019.

Christensen, N. S., and D. P. Lettenmaier (2007), A multimodel ensemble approach to assessment of climate change impacts on the hydrology and water resources of the Colorado River Basin, *Hydrol. Earth Syst. Sci.*, *11*(4), 1417–1434, doi:10.5194/hess-11-1417-2007.

Danczak, R. E., S. B. Yabusaki, K. H. Williams, Y. Fang, C. Hobson, and M. J. Wilkins (2016), Snowmelt induced hydrologic perturbations drive dynamic microbiological and geochemical behaviors across a shallow Riparian Aquifer, *Front. Earth Sci.*, *4*, 57, doi:10.3389/feart.2016.00057.

Dini-Andreote, F., J. C. Stegen, J. D. van Elsas, and J. F. Salles (2015), Disentangling mechanisms that mediate the balance between stochastic and deterministic processes in microbial succession, *Proc. Natl. Acad. Sci. U.S.A.*, *112*(11), E1326–E1332, doi:10.1073/pnas.1414261112.

Fasching, C., A. J. Ulseth, J. Schelker, G. Steniczka, and T. J. Battin (2016), Hydrology controls dissolved organic matter export and composition in an Alpine stream and its hyporheic zone, *Limnol. Oceanogr.*, *61*(2), 558–571, doi:10.1002/lno.10232.

Febria, C. M., R. R. Fulthorpe, and D. D. Williams (2010), Characterizing seasonal changes in physicochemistry and bacterial community composition in hyporheic sediments, *Hydrobiologia*, *647*(1), 113–126, doi:10.1007/s10750-009-9882-x.

Febria, C. M., P. Beddoes, R. R. Fulthorpe, and D. D. Williams (2012), Bacterial community dynamics in the hyporheic zone of an intermittent stream, *ISME J.*, *6*(5), 1078–1088, doi:10.1038/ismej.2011.173.

Feris, K. P., P. W. Ramsey, C. Frazar, M. C. Rillig, J. E. Gannon, and W. E. Holben (2003), Structure and seasonal dynamics of hyporheic zone microbial communities in free-stone rivers of the eastern United States, *Microb. Ecol.*, *46*(2), 200–215, doi:10.1007/BF03036883.

Feris, K. P., P. W. Ramsey, C. Frazar, M. Rillig, J. N. Moore, J. E. Gannon, and W. E. Holben (2004), Seasonal dynamics of shallow-hyporheic-zone microbial community structure along a heavy-metal contamination gradient, *Appl. Environ. Microbiol.*, *70*(4), 2323–2331, doi:10.1128/AEM.70.4.2323-2331.2004.

Ficklin, D. L., I. T. Stewart, and E. P. Maurer (2013), Climate change impacts on streamflow and subbasin-scale hydrology in the Upper Colorado River Basin, *PLoS One*, *8*(8), e71297, doi:10.1371/journal.pone.0071297.

Findlay, S., D. Strayer, C. Goumbala, and K. Gould (1993), Metabolism of streamwater dissolved organic carbon in the shallow hyporheic zone, *Limnol. Oceanogr.*, *38*(7), 1493–1499.

Findlay, S. E. G., R. L. Sinsabaugh, W. V. Sobczak, and M. Hoostal (2003), Metabolic and structural response of hyporheic microbial communities to variations in supply of dissolved organic matter, *Limnol. Oceanogr.*, *48*(4), 1608–1617, doi:10.4319/lo.2003.48.4.1608.

Fischer, H., A. Sachse, C. E. W. Steinberg, and M. Pusch (2002), Differential retention and utilization of dissolved organic carbon by bacteria in river sediments, *Limnol. Oceanogr.*, *47*(6), 1702–1711.

Fischer, H., F. Kloep, S. Wilzcek, and M. T. Pusch (2005), A river's liver - microbial processes within the hyporheic zone of a large lowland river, *Biogeochemistry*, *76*, 349–371, doi:10.1007/s10533-005-6896-y.

Francis, B. A., L. K. Francis, and M. B. Cardenas (2010), Water table dynamics and groundwater-surface water interaction during filling and draining of a large fluvial island due to dam-induced river stage fluctuations, *Water Resour. Res.*, *46*, W07513, doi:10.1029/2009WR008694.

Hartland, A., J. R. Larsen, M. S. Andersen, M. Baalousha, and D. O'Carroll (2015), Association of arsenic and phosphorus with iron nanoparticles between streams and aquifers: Implications for arsenic mobility, *Environ. Sci. Technol.*, *49*(24), 14,101–14,109, doi:10.1021/acs.est.5b03506.

Hester, E. T., K. I. Young, and M. A. Widdowson (2013), Mixing of surface and groundwater induced by riverbed dunes: Implications for hyporheic zone definitions and pollutant reactions, *Water Resour. Res.*, *49*, 5221–5237, doi:10.1002/wrcr.20399.

Holmes, D. E., K. T. Finneran, and D. R. Lovley (2002), Enrichment of Geobacteraceae associated with stimulation of dissimilatory metal reduction in uranium-contaminated aquifer sediments, *Appl. Environ. Microbiol.*, *68*, 2300–2306.

Holmes, D. E., L. Giloteaux, M. Barlett, A. Chavan, J. A. Smith, K. H. Williams, P. Long, and D. R. Lovley (2013), Molecular analysis of the in situ growth rates of subsurface, *Appl. Environ. Microbiol.*, doi:10.1128/AEM.03263-12.

Krause, S., D. M. Hannah, J. H. Fleckenstein, C. M. Heppell, D. Kaeser, R. Pickup, G. Pinay, A. L. Robertson, and P. J. Wood (2011), Inter-disciplinary perspectives on processes in the hyporheic zone, *Ecohydrology*, *4*(4), 481–499, doi:10.1002/eco.176.

Lovley, D. R., and E. J. P. Phillips (1986), Organic matter mineralization with reduction of ferric iron in anaerobic sediments, *Appl. Environ. Microbiol.*, *51*, 683–689.

McCallum, J. L., and M. Shanafield (2016), Residence times of stream-groundwater exchanges due to transient stream stage fluctuations, *Water Resour. Res.*, *52*, 2059–2073, doi:10.1002/2015WR017441.

Miller, M. P., D. D. Susong, C. L. Shope, V. M. Heilweil, and B. J. Stolp (2014), Continuous estimation of baseflow in snowmelt-dominated streams and rivers in the Upper Colorado River Basin: A chemical hydrograph separation approach, *Water Resour. Res.*, *50*, 6986–6999, doi:10.1002/2013WR014939.

Morrison, S. J., C. S. Goodknight, A. D. Tigar, R. P. Bush, and A. Gil (2012), Naturally occurring contamination in the Mancos Shale, *Environ. Sci. Technol.*, *46*(3), 1379–1387, doi:10.1021/es203211z.

Nagorski, S. A., and J. N. Moore (1999), Arsenic mobilization in the hyporheic zone of a contaminated stream, *Water Resour. Res.*, *35*, 3441–3450, doi:10.1029/1999WR900204.

Nowinski, J. D., M. B. Cardenas, A. F. Lightbody, T. E. Swanson, and A. H. Sawyer (2012), Hydraulic and thermal response of groundwater–surface water exchange to flooding in an experimental aquifer, *J. Hydrol.*, *472–473*, 184–192, doi:10.1016/j.jhydrol.2012.09.018.

Painter, T. H., J. S. Deems, J. Belnap, A. F. Hamlet, C. C. Landry, and B. Udall (2010), Response of Colorado River runoff to dust radiative forcing in snow, *Proc. Natl. Acad. Sci. U.S.A.*, *107*(40), 17,125–17,130, doi:10.1073/pnas.0913139107.

Petchey, O. L., and K. J. Gaston (2002), Functional diversity (FD), species richness and community composition, *Ecol. Lett.*, *5*(3), 402–411, doi:10.1046/j.1461-0248.2002.00339.x.

Sawyer, A. H., and M. B. Cardenas (2012), Effect of experimental wood addition on hyporheic exchange and thermal dynamics in a losing meadow stream, *Water Resour. Res.*, *48*, W10537, doi:10.1029/2011WR011776.

Shannon, C. (1948), A mathematical theory of communication, *Bell Syst. Tech. J.*, *27*, 379–423.

Stegen, J. C., X. Lin, A. E. Konopka, and J. K. Fredrickson (2012), Stochastic and deterministic assembly processes in subsurface microbial communities, *ISME J.*, *6*, 1653–1664, doi:10.1038/ismej.2012.22.

Stegen, J. C., X. Lin, J. K. Fredrickson, X. Chen, D. W. Kennedy, C. J. Murray, M. L. Rockhold, and A. Konopka (2013), Quantifying community assembly processes and identifying features that impose them, *ISME J.*, *7*, 2069–2079.

Stegen, J. C., X. Lin, J. K. Fredrickson, and A. E. Konopka (2015), Estimating and mapping ecological processes influencing microbial community assembly, *Front. Microbiol.*, *6*, 370, doi:10.3389/fmicb.2015.00370.

Stegen, J. C., et al. (2016), Coupled microbiome-biogeochemical responses to groundwater-surface water mixing, *Nat. Commun.*, *7*, 11237, doi:10.1038/ncomms11237.

Storey, R. G., D. D. Williams, and R. R. Fulthorpe (2004), Nitrogen processing in the hyporheic zone of a pastoral stream, *Biogeochemistry*, *69*(3), 285–313, doi:10.1023/B:BIOG.0000031049.95805.ec.

Stucker, V. K., K. H. Williams, M. J. Robbins, and J. F. Ranville (2013), Arsenic geochemistry in a biostimulated aquifer: An aqueous speciation study: Arsenic geochemistry in a biostimulated aquifer, *Environ. Toxicol. Chem.*, *32*(6), 1216–1223, doi:10.1002/etc.2155.

Tillman, F. D., S. Gangopadhyay, and T. Pruitt (2016), Changes in groundwater recharge under projected climate in the upper Colorado River basin, *Geophys. Res. Lett.*, *43*, 6968–6974, doi:10.1002/2016GL069714.

Wagner, K., M. M. Bengtsson, K. Besemer, A. Sieczko, N. R. Burns, E. R. Herberg, and T. J. Battin (2014), Functional and structural responses of hyporheic biofilms to varying sources of dissolved organic matter, *Appl. Environ. Microbiol.*, *80*(19), 6004–6012, doi:10.1128/AEM.01128-14.

Wilkins, M. J., et al. (2009), Proteogenomic monitoring of *Geobacter* physiology during stimulated uranium bioremediation, *Appl. Environ. Microbiol.*, *75*, 6591–6599, doi:10.1128/AEM.01064-09.

Williams, K. H., et al. (2011), Acetate availability and its influence on sustainable bioremediation of uranium-contaminated groundwater, *Geomicrobiol. J.*, *28*(5–6), 519–539, doi:10.1080/01490451.2010.520074.

Wong, J. C. Y., and D. D. Williams (2010), Sources and seasonal patterns of dissolved organic matter (DOM) in the hyporheic zone, *Hydrobiologia*, *647*(1), 99–111.

Xie, X., T. M. Johnson, Y. Wang, C. C. Lundstrom, A. Ellis, X. Wang, M. Duan, and J. Li (2014), Pathways of arsenic from sediments to groundwater in the hyporheic zone: Evidence from an iron isotope study, *J. Hydrol.*, *511*, 509–517, doi:10.1016/j.jhydrol.2014.02.006.

Yabusaki, S. B., Y. Fang, K. H. Williams, C. J. Murray, A. L. Ward, R. D. Dayvault, S. R. Waichler, D. R. Newcomer, F. A. Spane, and P. E. Long (2011), Variably saturated flow and multicomponent biogeochemical reactive transport modeling of a uranium bioremediation field experiment, *J. Contam. Hydrol.*, *126*(3–4), 271–290, doi:10.1016/j.jconhyd.2011.09.002.

Zarnetske, J. P., R. Haggerty, S. M. Wondzell, and M. A. Baker (2011), Dynamics of nitrate production and removal as a function of residence time in the hyporheic zone, *J. Geophys. Res.*, *116*, G01025, doi:10.1029/2010JG001356.